Articles

Theoretical Study of Ladder Polysilanes

Monica Kosa, Miriam Karni,* and Yitzhak Apeloig*

The Schulich Faculty of Chemistry and the Lise Meitner-Minerva Center for Computational Quantum Chemistry, Technion-Israel Institute of Technology, Haifa 32000, Israel

Received November 9, 2006

The parent ladder polysilanes $R_4Si_2-(Si_2R_2)_n-Si_2R_4$ (R = H, $n = 0-7$), composed of a catenation of cyclotetrasilane rings, and their corresponding methyl- (R = CH_3) and silyl-substituted (R = SiH_3) derivatives were studied computationally using quantum mechanical methods, mainly density functional theory. The calculations show that the parent ladder polysilanes have puckered four-membered rings for $n = 0-3$, 5 and nearly planar rings for $n = 4$, 6, 7 and, consequently, the parent ladder polysilanes are not twisted. In contrast, methyl- and silyl-substituted ladder polysilanes have twisted four-membered rings and the ladder is helical. This is consistent with experimental data for R = *i*Pr, which show twisting at each tetrasilacyclobutane ring, leading to a helical ladderane structure. The electronic properties of ladder polysilanes are similar to those of oligosilanes with the same number of Si−Si σ bonds. Upon chain elongation, the HOMO−LUMO gap decreases, reaching a gap of ca. 3.4 eV for $n = 7$ and ca. 2.3−2.7 eV, approaching the semiconductor range, when extrapolated to the polymeric limit, significantly smaller than the gap of 4.7 eV obtained computationally for regular polysilanes. These trends found computationally are consistent with the experimental UV−vis lowest energy transitions, which show a shift to longer wavelengths as the ladder is elongated.

Introduction

Polysilanes, Si_nR_{2n+2}, have unique electronic properties which make them useful in various electronic applications such as nonlinear optics, electric conduction and photoconduction, electroluminescence, light-emitting diodes, photoinitiation of polymerization, microlithography, and sensors.[1] Ladder polysilanes (e.g., **1**−**4**), which are the topic of this paper, constitute a family of polysilanes where two polysilane chains are connected by bridging Si−Si σ bonds.

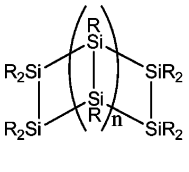

1, R = H, n = 0–7
2, R = Me, n = 0–7
3, R = SiH_3, n = 0–7
4, R = *i*Pr, n = 0–7

The aforementioned applications of polysilanes (as well as potential applications of ladder polysilanes) result from their unique electronic properties, which differ significantly from those of their carbon analogues. Gilman et al. were the first to report already in 1964 that permethylated silane oligomers, unlike the corresponding carbon systems, absorb strongly in the UV spectral region.[2] The exceptional features of the electronic spectra of polysilanes indicate the existence of significant orbital interactions and electronic delocalization within the framework of the σ bonds. The degree of electron delocalization in the backbone is a function of the β_{gem}/β_{vic} ratio, where β_{vic} is the interaction responsible for the Si−Si σ bond formation and β_{gem} is the interaction between two sp^3 hybrides located on the same silicon atom, as shown in Figure 1.[1a] If β_{gem}/β_{vic} vanishes, a complete localization of bonding and antibonding orbitals between pairs of silicon atoms exists. On the other hand, β_{gem}/β_{vic} equals unity when the delocalization is perfect. A well-known analogy is the isoelectronic π system of polyenes. When the C−C bond lengths in a polyene are all equal, all resonance integrals are equal and perfect delocalization results. When the bond lengths alternate, so will the resonance integrals, and the π components of the double bonds will be partially localized.[1a]

The orbital energies of oligosilanes and polysilanes are very sensitive to the molecular conformation.[1c] The dependence of the orbital energies on the SiSiSiSi dihedral angle is related to the difference between gauche and antiperiplanar orbital interactions.[3] In the antiperiplanar conformation (Figure 1a, ∠SiSiSiSi = 180°) $\beta_{14} > 0$, destabilizing the HOMO (which has a node at each silicon atom) and stabilizing the LUMO. In a gauche conformation where ∠SiSiSiSi = 60° (Figure 1b), the 1−4-

* To whom correspondence should be addressed. E-mail: chrapel@tx.technion.ac.il (Y.A.); chrmiri@tx.technion.ac.il (M.K.).

(1) (a) Miller, R. D.; Michl, J. *Chem. Rev.* **1989**, *89*, 1359. (b) Kira, M. In *Chemistry of Organic Silicon Compounds*; Rappoport, Z., Apeloig, Y., Eds.; Wiley: Chichester, U.K., 1998; Vol. 2, p 1311. (c) Fogarthy, H. A.; Casher, D. L.; Imhof, R.; Schepers, T.; Rooklin, D. W.; Michl, J. *Pure Appl. Chem.* **2003**, *75*, 999. (d) Kira, M., Ramachandram, B. In *The Handbook of Photochemistry and Photobiology*;Nalwa, H. S., Ed.; American Scientific: Stevenson Ranch, CA, 2003; Vol. 1, p 83. (e) Tsuji, H.; Michl, J.; Tamao, K. *J. Organomet. Chem.* **2003**, *685*, 9.

(2) (a) Gilman, H.; Atwell, W. H.; Schweke, G. L. *Chem. Ind.* (*London*) **1964**, 1063. (b) Gilman, H.; Atwell, W, H.; Schweke, G. L. *J. Organomet. Chem.* **1964**, *2*, 369.

(3) Plitt, H.; Downing, J. W.; Raymond, M. K., Balaji, V.; Michl, J. *J. Chem. Soc., Faraday Trans.* **1994**, *90*, 1653.

10.1021/om0610344 CCC: $37.00 © 2007 American Chemical Society
Publication on Web 04/19/2007

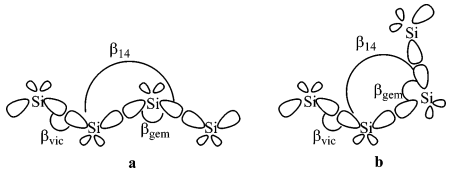

Figure 1. A σ conjugated linear chain of interacting $3sp^3$ silicon orbitals in a polysilane: (a) anti conformation; (b) gauche conformation.

interaction stabilizes the HOMO and destabilizes the LUMO.[4] Due to the low torsional barrier in polysilanes, conformations other than the usual anti ($\angle$SiSiSiSi = 180°) or gauche ($\angle$SiSiSiSi = 60°) may have an important contribution to the polysilane structure, consequently affecting its electronic properties.[5]

Substituents affect the electronic properties of oligosilanes because they interact with the HOMO and the LUMO and thus change the HOMO−LUMO gap. Such substituent effects were demonstrated by spectral (UV) and electrochemical measurements. For example, the measured oxidation potentials of a variety of alkyl polysilanes are in the range of 1.4−1.6 V (vs the saturated calomel electrode) and are relatively insensitive to the identity of the specific alkyl substituent.[6] However, aryl substitution at the polysilane backbone, as in poly(methylphenylsilane), reduces the oxidation potential by ~0.4−1.0 V, in agreement with the expectation that the interaction of the phenyl π system with the HOMO (Si−Si σ orbitals along the molecular backbone) destabilizes this orbital.[1a,5] Substitution of the phenyl ring with a *p*-OMe electron donor further reduces the oxidation potential of the polysilane.[5] The destabilization of the HOMO of aryl-substituted polysilanes is consistent with the observed red shifts of the UV absorption bands.[7]

Ladder polysilanes, $R_4Si_2-(Si_2R_2)_n-Si_2R_4$ (n = 0−7), first synthesized in 1987 by Matsumoto et al.,[8] constitute a class of polysilane compounds featuring a systematic catenation of cyclotetrasilane rings. A special feature of ladder polysilanes is the fact that their conformations are fixed, in contrast to the case for single-chain polysilanes, which have a highly flexible backbone. The most stable conformer is the all-anti conformer.

Ladder polysilanes show relatively strong absorption in the UV−visible region. In the series of the anti ladder polysilanes, **4** (R = iPr, n = 1−7), the lowest energy absorption maximum shifts progressively to longer wavelengths as the number of cyclotetrasilane rings increases from 2 to 8: i.e., λ = 310, 345, 380, 414, 440, 464, 483 nm, respectively. A similar bathochromic shift has been reported in analogous permethylpolysilanes.[1b] The ladder polysilanes also exhibit strong electron-donating properties. The oxidation potentials of the anti ladder polysilanes decrease slightly as the number of cyclotetrasilane rings increases. This trend in the oxidation potentials was attributed to destabilization of the HOMO upon the extension of the number of rings and consequently to a more efficient σ conjugation.[8b] A one-electron reduction of the ladder polysilanes **4** (n = 1−4) by early alkali metals, such as potassium and lithium, leads to the formation of the corresponding stable anion radicals, which persist for several months even at room temperature. Very recently, ladder polysilanes were recognized as stable building blocks of tetragonal single-walled silicon nanotubes.[9] Calculations showed that single-walled silicon nanotubes have zero band gap, suggesting that they are better described as metals rather than wide-gap semiconductors.[10]

Analogous carbon ladderanes are known,[11] and they are promising building blocks in optoelectronics.[12] However, their electronic properties are very different from those of ladder polysilanes. Carbon ladderanes have also been identified in biological systems in the form of ladderane lipids, which are integral components in the microbiological conversion of ammonium and nitrite ions to dinitrogen gas.[13] Carbon ladderanes were recognized as possible fluxional molecules: e.g., sigmatropic shiftamers.[14] Sigmatropic shiftamers were originally conceived as hydrocarbon polymers in which localized bonds could be transported back and forth along the polymer chain via sequential [3,3]-sigmatropic shifts.[14b] In ladderanes, a pair of parallel π bonds (derived in a "gedank experiment" from a retro [2 + 2] reaction of one of the cyclobutane rings of the polymer) was envisioned as the bonding unit that would move along the polymer chain via Cope rearrangement.[14]

Despite the accumulated experimental data and the potential applications of ladder polysilanes, the theoretical information regarding this important group of compounds is very limited, in contrast to the many studies of carbon ladderanes.[14] In view of the recent synthetic achievements in the synthesis and characterization of ladder polysilanes,[8] we have studied computationally a series of ladder polysilanes and present here an extensive theoretical study of their geometries and electronic properties. The specific systems that were studied computationally include $R_4Si_2-(Si_2R_2)_n-Si_2R_4$ (R = H, Me, SiH_3 with n = 0−7): i.e., **1**−**3**. These theoretical studies are important for broadening the fundamental knowledge of these important materials as well as for predicting the properties of yet unknown molecules of this family of compounds.

Computational Methods

Calculations were performed using both ab initio[15] and density functional theory (DFT)[16] methods, as implemented in the Gaussian 03 series of programs.[17] The geometries of all molecules were fully optimized, and vibrational frequencies were computed at the same level in order to characterize the stationary points as minima (no

(4) The sensitivity to twisting displayed by a given MO depends significantly on the degree of its 3s vs 3p character, since only the 3p contribution responds to twisting. Thus, the HOMO, which has nearly a pure $3p_z$ character, is very sensitive to twisting, while the LUMO, which has a high 3s character, is considerably less sensitive to twisting.[1a]

(5) (a) Plitt, H. S.; Downing, J. W.; Raymond, M. K.; Balaji, V.; Michl, J. *J. Chem. Soc., Faraday Trans.* **1995**, *90*, 1653. (b) Albinsson, B.; Antic, D.; Neumann, F.; Michl, J. *J. Phys. Chem. A* **1999**, *103*, 2184.

(6) Diaz, A.; Miller, R. D. *J. Electrochem. Soc.* **1985**, *132*, 834.

(7) Trefonas, P.; West, R.; Miller, R. D.; Hofer, D. *J. Polym. Sci., Polym. Lett. Ed.* ***1983***, *21*, 823.

(8) (a) Matsumoto, H.; Miyamoto, H.; Kojima, N.; Nagai, Y. *J. Chem. Soc., Chem. Commun.* **1987**, 1316. (b) Kyushin, S.; Matsumoto, H. *Adv. Organomet. Chem.* **2003**, *49*, 133. (c) Kyushin, S.; Ueta, Y.; Tanaka, R.; Matsumoto, H. *Chem. Lett.* **2006**, *35*, 182.

(9) Perepichka, D. F.; Rosei, F. *Small* **2006**, *2*, 22.

(10) Bai, J.; Zeng, X. C.; Tanaka, H.; Zeng, J. Y. *Proc. Natl. Acad. Sci. U.S.A.* **2004**, *101*, 2664.

(11) For a recent highlight, see: Hopf, H. *Angew. Chem., Int. Ed.* **2003**, *42*, 2822.

(12) Li, W.; Fox, M. A. *J. Am. Chem. Soc.* **1996**, *118*, 11752.

(13) (a) DeLong, E. F. *Nature* **2002**, *419*, 676. (b) Damste, J. S. S.; Strous, M.; Rijpstra, W. I. C.; Hopmans, E. C.; Geenevasen, J. A. J.; van Duin, A. C. T.; van Niftrik, L. A.; Jetten, M. S. M. *Nature* **2002**, *419*, 708.

(14) (a) For a review of this topic see: Tantillo, D. J.; Hoffmann, R. *Acc. Chem. Res.* **2006**, *39*, 477. (b) Tantillo, D. J.; Hoffmann, R. *Angew. Chem., Int. Ed.* **2002**, *41*, 1033.

(15) (a) Hehre, J. W.; Radom, L.; Schleyer, P. v. R.; Pople, J. A. *Ab initio Molecular Orbital Theory*; Wiley: New York, 1986. (b) Young, D. C. *Computational Chemistry*; Wiley: New York, 2001. (c) Jensen, F. *Introduction to Computational Chemistry*; Wiley: Chichester, U.K., 1999.

(16) (a) Parr, R. G.; Yang, W. *Density Functional Theory of Atoms and Molecules*; Oxford University Press: Oxford, U.K., 1989. (b) Koch. W.; Holthausen, M. C. *A Chemist's Guide to Density Functional Theory*; Wiley-VCH: Weinheim, Germany, 2000. (c) Becke, A. D. *Phys. Rev. A* **1988**, *38*, 3098. (d) Lee, C.; Yang, W.; Parr, R. G. *Phys. Rev. B* **1988**, *37*, 785.

imaginary eigenvalues) or transition states (one imaginary eigenvalue). Both DFT and ab initio methods were used for geometry optimizations. For the DFT calculations we used the hybrid-density B3LYP[16c,d] functional with the 6-31G(d) basis set (designated as B3LYP/6-31G(d)//B3LYP/6-31G(d)). Larger basis sets of a triple-ζ type, which also included diffuse functions, e.g., 6-311+G(d), have only a small effect on the geometry and the HOMO−LUMO gaps (see Tables S1 and S2 in the Supporting Information). Ab initio calculations were performed at the correlated MP2/6-31G(d)//MP2/6-31G(d) level of theory. For calculating the lowest energy UV−vis transitions, we have used the TDB3LYP[18]/6-311++G(d,p)//B3LYP/6-31G(d) method, which was previously shown to produce results which are in better agreement with the experimental values than those calculated by the CIS method, both for organic and for organosilicon compounds.[19]

The discussion of the geometries and energies is based on the B3LYP/6-31G(d)//B3LYP/6-31G(d)) calculations, unless stated otherwise.

Results and Discussion

The ladder polysilanes which were studied are **1**−**3** (n = 0−7). The polysilanes **2** (R = Me) are models for the experimentally studied ladder polysilanes **4** (R = *i*Pr).

1. Geometry. Chart 1 shows the notations of the geometrical parameters for **1**−**4**.

Chart 1

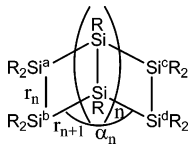

The Si−Si bond lengths and the SiSiSi bond angles of **1**−**3** are quite regular, with no outstanding features relative to chain polysilanes. The longitudinal Si−Si bonds, r_{n+1}, are ca. 2.37 Å, and the bridging Si−Si bonds, r_n, are longer at around 2.42 Å. The SiSi bond lengths in corresponding oligosilanes are somewhat shorter: ca. 2.35 Å. The SiSiSi bond angles along the ladderane chain are nearly constant at ca. 112°—the same angle as in the parent (all-trans) oligosilane chain, $-(SiH_2)_n-$.

The most interesting geometrical features are the puckering angles of the four-membered rings and the degree of twisting (or helicity) of the ladder polysilane. Tables 1−3 (entries 1−8) show the SiSiSiSi dihedral angles for each of the four-membered rings present in the ladder polysilanes **1**−**3** (n = 0−7), respectively. For example, in the ladder polysilane **1** (n = 2), constituting three rings, the SiSiSiSi dihedral angle of the two outer rings are 9.7 and 9.8° (Table 1, entries 1 and 3) and the dihedral angle of the central ring is 8.4° (entry 2). The parent tetrasilacyclobutane **1** (n = 0) is not planar, having a SiSiSiSi dihedral angle of 22.5°. The square-planar ring structure (∠SiSiSiSi = 0°) is a transition structure interconnecting two equivalent puckered structures, and it is 0.9 kcal/mol higher in energy. The puckering dihedral angle of the tetrasilacyclobutane rings decreases as the number of rings increases and the barrier for planarization vanishes, being only 0.1 kcal/mol already for **1** (n = 2). Ladder polysilanes **1** (n = 4, 6, 7) have planar tetrasilacyclobutane rings, and in **1** (n = 5) the ring puckering angles range between 2.4 and 6.7° (Table 1). In each of the parent ladderanes the inner rings are less twisted than the external rings.

Table 1. Calculated (B3LYP/6-31G(d)) Puckering Angles (∠SiSiSiSi, in deg) within the Four-Membered Rings and the Degree of Helicity, *h*, of 1 (R = H, *n* = 0−7)

	n							
entry[a]	0	1	2	3	4	5	6	7
1	22.5	14.5	9.7	8.6	0.2	6.7	0.0	0.0
2		14.5	8.4	6.2	0.1	4.2	0.0	0.0
3			9.8	6.1	0.0	2.6	0.0	0.0
4				8.6	0.1	2.4	0.0	0.0
5					0.1	3.6	0.0	0.0
6						5.7	0.0	0.0
7							0.0	0.0
8							0.0	0.0
h	22.5	25.0	24.5	25.2	0.0	21.6	0.0	0.0

[a] Position of the ring along the ladder chain.

In the methyl- and silyl-substituted tetrasilacyclobutanes **2** (R = CH_3, n = 0) and **3** (R = SiH_3, n = 0) the puckering angles (∠SiSiSiSi) are 19.5 and 15.9°, respectively, smaller than the puckering angle in **1** (n = 0) (22.5°). Upon elongation of the ladders of **2** and **3** the puckering angle decreases to 11−14° (Tables 2 and 3), which is larger than in **1** (Table 1). The significant degree of puckering in **2** and **3** is consistent with the observed structures of the ladderanes **4** (R = *i*Pr, n = 1−7), which exhibit significant puckering of each of the tetrasilacyclobutane rings, leading eventually to helical structures.[8] For example, the experimental ranges of the SiSiSiSi dihedral angles of **4** (n = 5−7) are 22.8−29.8, 23.9−31.7, and 24.6−28.2°, respectively (Table 2, entry 10). The higher degree of puckering in **4** (R = *i*Pr) as compared to that in **2** (R = Me) probably reflects the larger size of the isopropyl substituents, which reduce their mutual steric repulsion by adopting a higher degree of puckering.

The puckering of each of the ladderane rings leads to its helicity. The degree of helicity can be measured by the dihedral angle ∠($Si^aSi^bSi^dSi^c$) between the external four silicon atoms of the ladder chain (Si^a, Si^b) and (Si^d, Si^c), as shown in Chart 1. This angle is designated as the helicity index, *h*, and can be approximated by the sum of the puckering angles of the individual inner rings along the ladder. In the parent ladderanes **1** (R = H), *h* is in the range of 22−25° for n = 0−3 and n = 5 but it is 0° for n = 4, 6, 7 (Table 1, entry 9). Thus, parent ladder polysilanes longer than n = 6 are predicted *not* to be helical. In the substituted ladderanes the puckering angles of each of the rings are almost constant, around 12° (Tables 2 and 3), and therefore the degree of helicity increases as the chain becomes longer. Thus, in the methyl- and silyl-substituted ladderanes **2** and **3**, respectively, the helicity *h* of the molecule increases significantly as the ladderane chain becomes longer (Tables 2 and 3). For **2** (R = CH_3, n = 1−7) *h* is 20.0, 33.6, 40.9, 53.6, 66.7, 74.8, and 88.1°. For **3** (R = SiH_3, n = 1−7) *h* is 16.7, 32.3, 42.8, 57.3, 72.1, 84.1, and 102.9°, respectively.

(17) Frisch, M. J.; Trucks, G. W.; Schlegel, H. B.; Scuseria, G. E.; Robb, M. A.; Cheeseman, J. R.; Montgomery, J. A., Jr.; Vreven, T.; Kudin, K. N.; Burant, J. C.; Millam, J. M.; Iyengar, S. S.; Tomasi, J.; Barone, V.; Mennucci, B.; Cossi, M.; Scalmani, G.; Rega, N.; Petersson, G. A.; Nakatsuji, H.; Hada, M.; Ehara, M.; Toyota, K.; Fukuda, R.; Hasegawa, J.; Ishida, M.; Nakajima, T.; Honda, Y.; Kitao, O.; Nakai, H.; Klene, M.; Li, X.; Knox, J. E.; Hratchian, H. P.; Cross, J. B.; Bakken, V.; Adamo, C.; Jaramillo, J.; Gomperts, R.; Stratmann, R. E.; Yazyev, O.; Austin, A. J.; Cammi, R.; Pomelli, C.; Ochterski, J. W.; Ayala, P. Y.; Morokuma, K.; Voth, G. A.; Salvador, P.; Dannenberg, J. J.; Zakrzewski, V. G.; Dapprich, S.; Daniels, A. D.; Strain, M. C.; Farkas, O.; Malick, D. K.; Rabuck, A. D.; Raghavachari, K.; Foresman, J. B.; Ortiz, J. V.; Cui, Q.; Baboul, A. G.; Clifford, S.; Cioslowski, J.; Stefanov, B. B.; Liu, G.; Liashenko, A.; Piskorz, P.; Komaromi, I.; Martin, R. L.; Fox, D. J.; Keith, T.; Al-Laham, M. A.; Peng, C. Y.; Nanayakkara, A.; Challacombe, M.; Gill, P. M. W.; Johnson, B.; Chen, W.; Wong, M. W.; Gonzalez, C.; Pople, J. A. *Gaussian 03*, revision C.02; Gaussian, Inc.: Wallingford, CT, 2004.

(18) Bauernschmitt, R.; Ahlrichs, R. *Chem. Phys. Lett*., **1996**, *256*, 454.

(19) Sharma, A.; Lourderaj, U.; Deepak Sathyamurthy, N. *J. Phys. Chem. B* **2005**, *109*, 15860.

Table 2. Calculated (B3LYP/6-31G(d)) Puckering Angles (∠SiSiSiSi, in deg) within the Four-Membered Rings and the Degree of Helicity, *h*, of 2 (R = CH_3, *n* = 0−7)

	n							
entry[a]	0	1	2	3	4	5	6	7
1	19.5	11.6	13.4	12.9	13.2	13.9	13.5	14.2
2		11.5	11.3	10.7	11.6	12.3	11.9	11.9
3			13.4	10.6	11.7	12.3	11.7	12.4
4				13.1	11.6	12.2	11.8	12.2
5					13.2	12.6	11.7	12.4
6						13.7	11.9	12.2
7							13.5	11.9
8								14.1
h	19.5	20.0	33.6	40.9	53.6	66.7	74.8	88.1
10[b]		21.4−21.8	22.6−25.2	24.5−27.1	23.8−28.8	22.8−29.8	23.9−31.7	24.6−28.2
11[c]						96.2	119.6	128.5

[a] Position of the ring along the ladder chain. [b] Range of ∠SiSiSiSi within the rings of **4** (*n* = 1−7).[8b,c] [c] *h* in **4**.

Table 3. Calculated (B3LYP/6-31G(d)) Puckering Angles (∠SiSiSiSi, in deg) within the Four-Membered Rings and the Degree of Helicity, *h*, of 3 (R = SiH_3, *n* = 0−7)

	n							
entry[a]	0	1	2	3	4	5	6	7
1	15.9	9.5	12.9	13.4	13.6	13.5	12.9	15.1
2		9.5	10.6	11.1	11.8	12.7	12.3	13.1
3			12.9	11.0	12.5	15.1	14.3	14.1
4				13.5	12.7	14.7	16.9	16.4
5					14.8	12.9	14.3	17.1
6						13.3	12.3	14.8
7							12.9	12.5
8								13.9
h	15.9	16.7	32.3	42.8	57.3	72.1	84.1	102.9

[a] Position of the ring along the ladder chain.

The helicity of the silyl-substituted ladderanes **3** is somewhat larger than that of the methyl-substituted ladders. Assuming a constant puckering of 12° of each of the rings in **2** and **3**, it can be predicted that in a ladder polysilane which consists of 15 rings *h* will be approximately 180°, thus completing a full cycle of the helix. In the experimentally known ladderanes **4** (*n* = 5−7) *h* is 96.2, 119.6, and 128.5°, respectively.[8c]

The calculations indicate clearly that the origin of the helicity in ladder polysilanes is steric, not electronic. This is suggested by the small degree of helicity of the parent ladderane **1** (*n* = 1−3, 5) and zero helicity in **1** (*n* = 4, 6, 7), as well as the similar helicities in **2** (R = Me) and **3** (R = SiH_3), although methyl and silyl substituents have very different electronic effects on the silicon skeleton.[20] More support for the role of steric effects comes from the fact that **2**, with a small alkyl substituent (Me), has a smaller degree of ring puckering (and eventually *h*), ca. 12°, than **4** with the larger substituent R = *i*Pr (Table 2), ca. 21.4−31.7°.

2. Molecular Orbitals of Ladder Polysilanes. The most important property with respect to possible applications of ladder polysilanes is their electronic structure, and it is therefore important to understand the shapes and the energies of their molecular orbitals. The energies of the HOMO and the LUMO as well as the HOMO−LUMO gap of **1**−**3** are given in Table 4.[21] The shapes of the HOMO and LUMO of **1** (*n* = 0−7) are shown in Figure 2.

The HOMOs of silicon ladderanes consist of a chain of σ bonding orbitals located on the two parallel silicon chains with a node at each silicon atom. A nodal plane also dissects the tetrasilacyclobutane rings along the ladderane. The shape of the HOMO of the corresponding oligosilanes is similar. The LUMO of the silicon ladderanes is localized in the regions above and below the bridging silicon−silicon bonds which connect the two oligosilane chains in the ladderane and has a bonding character there. It changes its sign along the chains at each bridging silicon−silicon bond. Thus, along each chain it can be viewed as having a pseudo π^* character.[22] The shape of these orbitals dictates that upon HOMO−LUMO excitation the bridging Si−Si bonds are shortened and strengthened while the Si−Si bonds along the chain are elongated and weakened. The shapes of these orbitals are similar to those of the isoelectronic carbon ladderanes.

Figure 3 shows a plot of the HOMO and LUMO orbital energies and the HOMO−LUMO energy gap for the parent silicon ladderanes **1** and those for the corresponding chain oligosilanes as well as the HOMO−LUMO energy gap of four carbon ladderanes. The relevant energies are also given in Table 4.

Silicon ladderanes constitute a subfamily of linear polysilanes, and their electronic properties therefore show similar trends upon chain elongation. In ladder polysilanes, the HOMO is destabilized from −7.1 eV in cyclotetrasilane **1** (*n* = 0) to −5.0 eV in **1** (*n* = 7) (Figure 3 and Table 4), while the LUMO is stabilized from −0.8 eV for **1** (*n* = 0) to −2.5 eV for **1** (*n* = 7). Consequently, the HOMO−LUMO gap in silicon ladderanes is reduced from 6.3 eV in tetrasilacyclobutane **1** (*n* = 0) to 3.4 eV in **1** (*n* = 7) — consisting of eight tetrasilacyclobutane rings. It is interesting that the HOMO−LUMO energy gap in **1** is reduced by a constant value of 0.2 eV for each additional ring from *n* = 4 to *n* = 7. These trends are similar to those found for linear oligosilanes, in which the HOMO is destabilized as the chain becomes longer (from −8.1 eV in $H_3Si-SiH_3$ (with one Si−Si bond) to −6.9 eV in nonasilane) and the LUMO is stabilized (from 0.5 to −1.3 eV, respectively, Figure 3 and Table 4). Consequently, the HOMO−LUMO gap is reduced by 3.1 eV, from 8.7 eV in disilane to 5.6 eV in nonasilane. Also in linear oligosilanes, from hexasilane onward, the HOMO−LUMO energy gap decreases by 0.2 eV for each additional SiH_2 unit. The overall change in the HOMO−LUMO gap on going

(20) Apeloig, Y. In *Chemistry of Organic Silicon Compounds*; Patai, S., Rappoport, Z., Eds.; Wiley: Chichester, U.K., 1989; p 57.

(21) (a) We use DFT Kohn−Sham (KS) orbitals. The energies of KS orbitals were discussed and compared to those calculated by HF and EH (extended Hückel) methods, and it was found that although the absolute energies of KS orbitals are very different from those calculated by HF and EH methods, a linear relationship exists between the DFT orbital energies and orbital energies calculated with other methods.[21b] Thus, for comparison purposes the KS orbital energies are valid. (b) Stowasser, R.; Hoffmann, R. *J. Am. Chem. Soc.* **1999**, *121*, 3414. (c) Good agreement was found between HOMO−LUMO gaps calculated at B3LYP/6-31G(d) and experimental values for oligothiphenes; see: Zade, S. S.; Bendikov, M. *Org. Lett.* **2006**, *8*, 5243.

(22) Nuspl, G.; Polborn, K.; Evers, J.; Landrum, G. A.; Hoffmann, R. *Inorg. Chem.* **1996**, *35*, 6922.

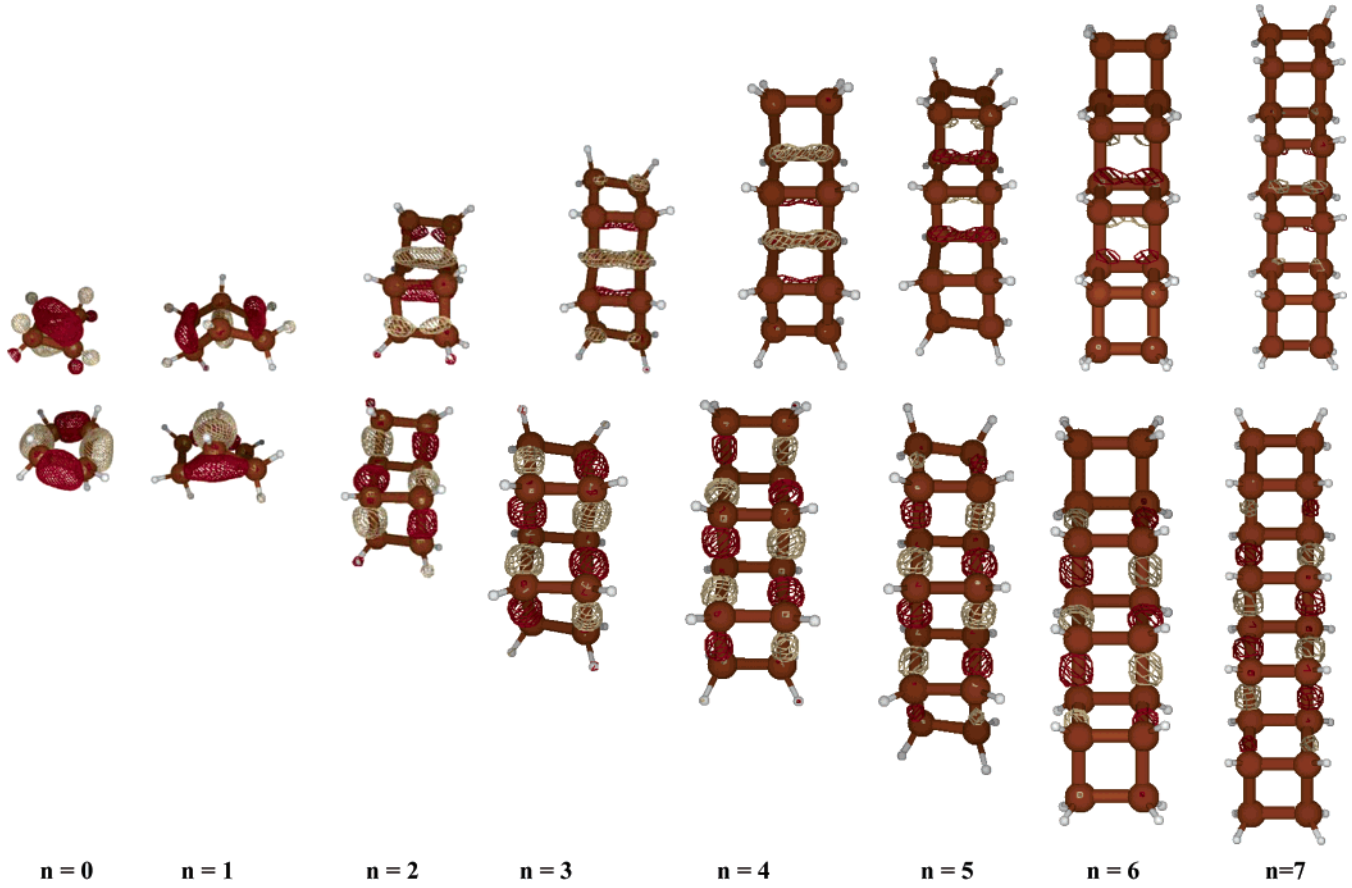

Figure 2. Calculated HOMO (bottom) and LUMO (top) molecular orbitals of **1** ($n = 0-7$).

Table 4. HOMO and LUMO Energies (eV)[21a,b] and HOMO−LUMO Energy Gaps (eV)[21] of 1−3 ($n = 0-7$) Calculated at B3LYP/6-31G(d)//B3LYP/6-31G(d)

	1 (R = H)			**2** (R = Me)			**3** (R = SiH_3)		
n	HOMO	LUMO	HOMO−LUMO	HOMO	LUMO	HOMO−LUMO	HOMO	LUMO	HOMO−LUMO
0	−7.1	−0.8	6.3	−5.6	−0.2	5.4	−6.9	−1.3	5.6
1	−6.9	−1.3	5.6	−5.6	−0.5	5.1	−6.6	−1.8	4.8
2	−6.6	−1.7	4.9	−5.4	−0.7	4.7	−6.5	−2.0	4.4
3	−6.4	−1.9	4.4	−5.2	−0.9	4.2	−6.3	−2.2	4.1
4	−6.2	−2.1	4.0	−5.0	−1.1	3.9	−6.2	−2.4	3.8
5	−6.0	−2.3	3.8	−4.9	−1.2	3.7	−6.2	−2.5	3.7
6	−5.9	−2.4	3.6	−4.8	−1.3	3.4	−6.1	−2.6	3.5
7	−5.8	−2.5	3.4	−4.7	−1.4	3.3	−6.1	−2.7	3.4

from $n = 0$ to $n = 7$ is ca. 3 eV, in both ladder polysilanes and chain polysilanes. A similar trend in the HOMO−LUMO gap was found for carbon ladderanes, where the HOMO−LUMO gap in cyclobutane of 10.6 eV is reduced to 8.3 eV for a carbon ladderane consisting of nine cyclobutane rings.[23] Substitution of the hydrogens of **1** by methyl groups (i.e., **2**) destabilizes both the HOMO and the LUMO and thus reduces only slightly the HOMO−LUMO gap. For example for **1** ($n = 4-7$) the HOMO−LUMO gaps are 4.0, 3.8, 3.6, and 3.4 eV, respectively, while those for **2** ($n = 4-7$) are 3.9, 3.7, 3.4, and 3.3 eV, respectively (Table 4). For the SiH_3-substituted ladder polysilanes **3**, both the HOMO and the LUMO are slightly stabilized relative to **1**, but the HOMO−LUMO gap remains practically unchanged relative to the corresponding **1** and **2**. Thus, we conclude that the HOMO−LUMO gap in ladder polysilanes is not sensitive to methyl or silyl substitution.

Extrapolation of the curve which describes the HOMO−LUMO energy gap as a function of $1/n$ to the polymeric limit ($1/n = 0$) predicts band gaps of 2.4, 2.3, and 2.7 eV for **1**−**3**, respectively, approaching the semiconductor range, and significantly smaller than the band gap of 4.7 eV calculated for $H_3Si\text{-}(SiH_2)_n\text{-}SiH_3$ by extrapolation to the polymeric limit.[24]

The most important difference between the carbon and the silicon ladderanes, which also dictates their different applications, is the fact that the HOMO−LUMO gap in silicon ladderanes is much smaller than in the corresponding carbon ladderanes (Figure 3). This is expected from the σ conjugation model, which shows that σ conjugation in oligosilane chains is significantly stronger than that in oligocarbon chains.[1] The much stronger σ conjugation is what makes oligosilanes in general and ladder polysilanes in particular so attractive for a variety of applications which are based on the relatively small HOMO−LUMO gap.[1,25]

3. Oxidation and Reduction of Ladder Polysilanes. HOMO energies are related to oxidation potentials. The measured oxidation potentials for **4** ($n = 0-4$) are 1.24, 0.87, 0.85, 0.82, and 0.74 V, respectively, vs SCE.[8b] This trend in the oxidation

(23) Santos, J. C.; Fuentealba, P. *Chem. Phys. Lett.* **2003**, *377*, 449.

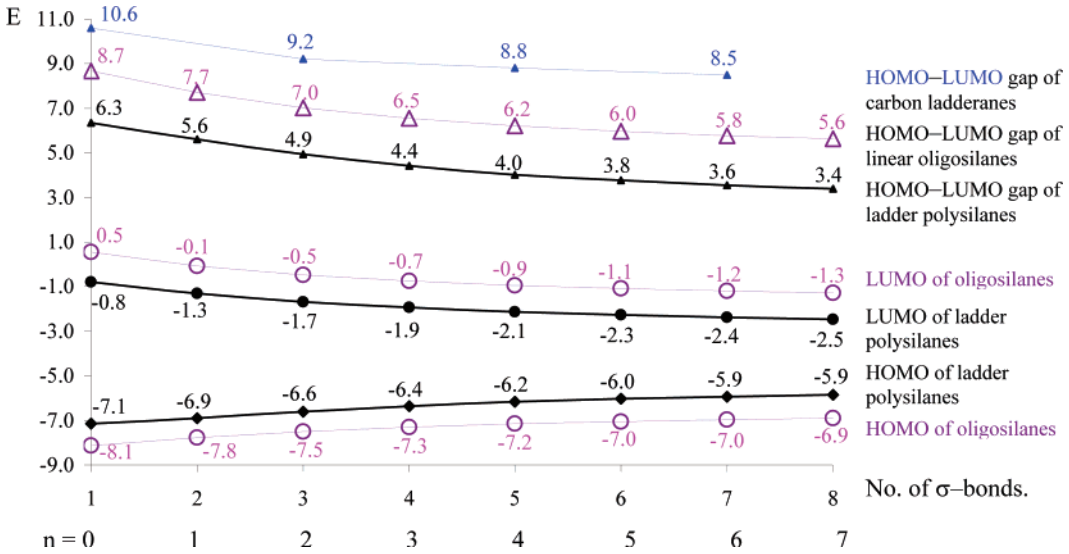

Figure 3. Calculated (B3LYP/6-31G(d)//B3LYP/6-31G(d)) HOMO and LUMO energies (in eV)[21a,b] of ladder polysilanes **1** (n = 0−7) and of linear oligosilanes $-(SiH_2)_n-$ (n = 0−7) and the corresponding HOMO−LUMO gaps (in eV), including those of several carbon ladderanes.

potentials is consistent with the trend in the calculated HOMO energies of **2** (n = 0−4), which are −5.6, −5.6, −5.4, −5.2, and −5.0 eV, respectively.

LUMO energies are related to reduction potentials. It was found experimentally that **4** (n = 1−4) are reduced with potassium to form stable radical anions, **4**$^{\bullet-}$ (n = 1−4), which were monitored by ESR.[8b] Radical anions **4**$^{\bullet-}$ (n = 1−4) become more stable as the number of cyclotetrasilane rings increases progressively. Thus, when a solution of **4**$^{\bullet-}$ (n = 1) generated at −70 °C was warmed above −10 °C, the ESR signal gradually decreased, but for **4**$^{\bullet-}$ (n = 4), the ESR signals remained persistent for several months at room temperature. Furthermore, **4**$^{\bullet-}$ (n = 4) could be generated also by treatment of **4** (n = 4) with lithium, a weaker reducing agent. These experimental findings are in agreement with the calculated very low LUMO energies of **2**, which are in the range of −0.2 and −1.4 eV for **2** (n = 0−7). Even lower LUMO energies are calculated for **1** and **3**, reaching values as low as −2.7 eV for **3** (n = 7), which indicates higher electron affinity for silyl-substituted ladder polysilanes[26] than for the corresponding alkyl-substituted ladder polysilanes.

The structure of the radical anions **4**$^{\bullet-}$ (n = 1−4) of ladder polysilanes is not known. Nevertheless, the oxidation of **4**$^{\bullet-}$ (n = 1−4) by O_2 recovered the initial ladder polysilanes **4** (n = 1−4) (eq 1), indicating that the radical anions of ladder polysilanes **4**$^{\bullet-}$ (n = 1−4) retain the ladder structure and that Si−Si bond cleavage or skeletal rearrangement does not occur.

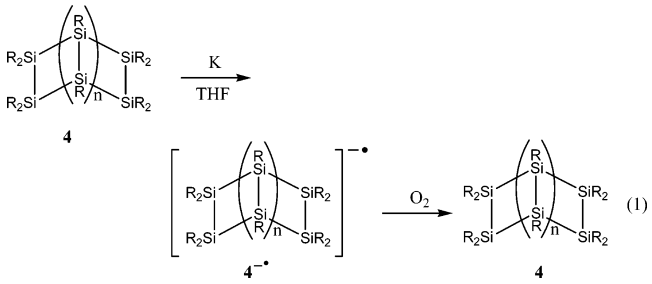

We have studied computationally the geometry and electronic structure of stable radical anions of ladder polysilanes, **2**$^{\bullet-}$ (n = 1−4).

Calculations[27] of model compounds **2**$^{\bullet-}$ (n = 1−4) (Figure 4) show that the general structure of ladderane is retained upon oxidation of **2** (n = 1−4) to **2**$^{\bullet-}$ (n = 1−4) and no Si−Si bonds are broken, in agreement with the experimental finding described above.[8] However, the geometrical parameters such as bond lengths and dihedral angles of **2**$^{\bullet-}$ (n = 1−4) differ significantly from those of the corresponding neutral ladderanes. Comparison between the bond lengths of **2** (n = 2−4) and **2**$^{\bullet-}$ (n = 2−4) (Figure 4) reveals that in general, upon reduction, the longitudinal Si−Si bonds are elongated while the bridging Si−Si bonds are shortened. For example, the inner longitudinal bond lengths of **2**$^{\bullet-}$ (n = 4) are ca. 2.41 Å, while the bridging bonds are ca. 2.38 Å. The corresponding bond lengths in **2** (n = 4) are 2.39 and 2.41 Å, respectively. The elongation of the longitudinal bonds and shortening of the bridging bonds is consistent with the shape of the LUMO (which accepts an additional electron) having an antibonding character between the two longitudinal silicon atoms and a bonding character between the bridging silicon atoms (Figure 1).

(24) (a) The graphs that describe the correlation between the HOMO−LUMO gaps and the reciprocal of the number of repeat units n (1/n), for ladder polysilanes **1**−**3**, for H_3Si-$(SiH_2)_n$-SiH_3 (n = 2−7) and for carbon ladderanes with n = 2−4, fit a quadratic function (with R^2 = 0.9977, 0.9937, 0.9953, 0.9942 and 1.0, respectively, for details see Figure 1S in the Supporting Information). A linear correlation exhibited a somewhat poorer fit (R^2 = 0.977, 0.969, 0.963 and 0.975 for **1**−**3** and oligosilanes, respectively). A quadratic correlation was also used for the extrapolation of the HOMO−LUMO gaps of conjugated oligomers to the polymeric limit.[21c] (b) A band-gap of 8.1 eV was previously calculated for a ladder polysilane (R = H) by a one dimensional tight-binding self-consistent-field crystal orbital (SCF-CO) method. However, the authors commented that this band-gap is highly over-estimated, by a factor of 3−4: Yamaguchi, Y.; Shioya, J. *Synthetic Mat.* **1993**, *59*, 29.

(25) For a recent highlight on the construction of molecules with a small HOMO−LUMO gap, see: Perepichka, D. F.; Bryce, M. R. *Angew. Chem., Int. Ed.* **2005**, *44*, 5370.

(26) Kyushin, S.; Miyajima, Y.; Matsumoto, H. *Chem. Lett.* **2000**, *29*, 1420.

(27) **2**$^{\bullet-}$ (n = 1) was calculated also using a larger basis set, including diffuse functions, at the UB3LYP/6-31G+(d) level. At this level of theory, the three bridging Si-Si bond lengths are 2.381, 2.363, and 2.381 Å, while the longitudinal Si−Si bonds are 2.385 and 2.376 Å. Increasing the basis set from 6-31G(d) to 6-31G+(d) shortens the bridging Si−Si bonds while lengthening the longitudinal Si−Si bonds.

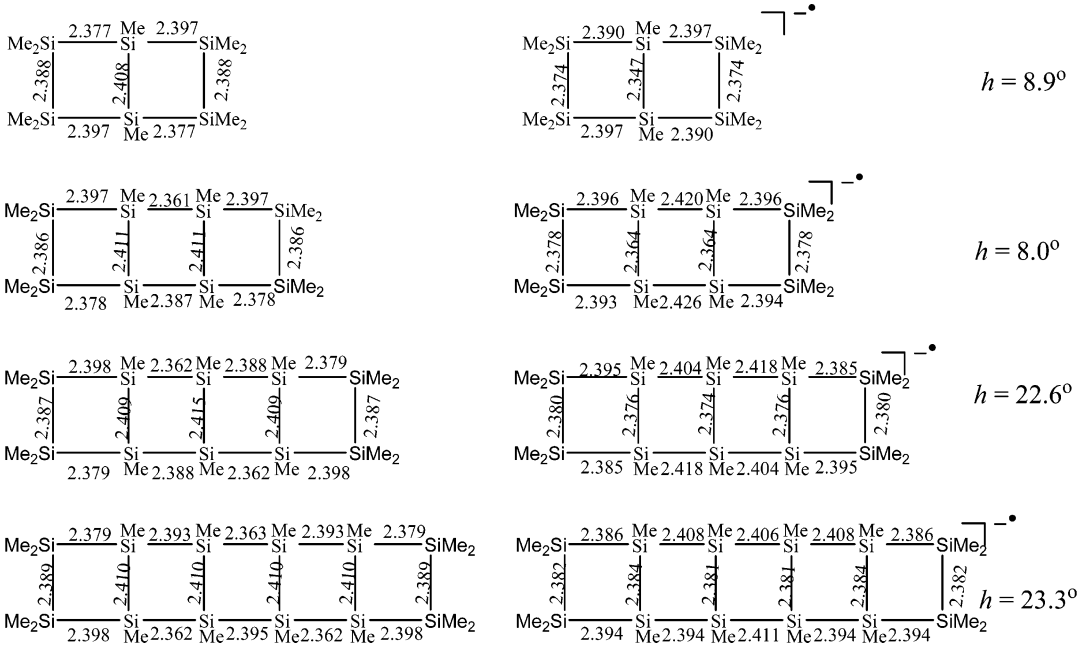

Figure 4. Calculated bond lengths in **2** (n = 1−4) and in **2**$^{\bullet-}$ (n = 1−4).

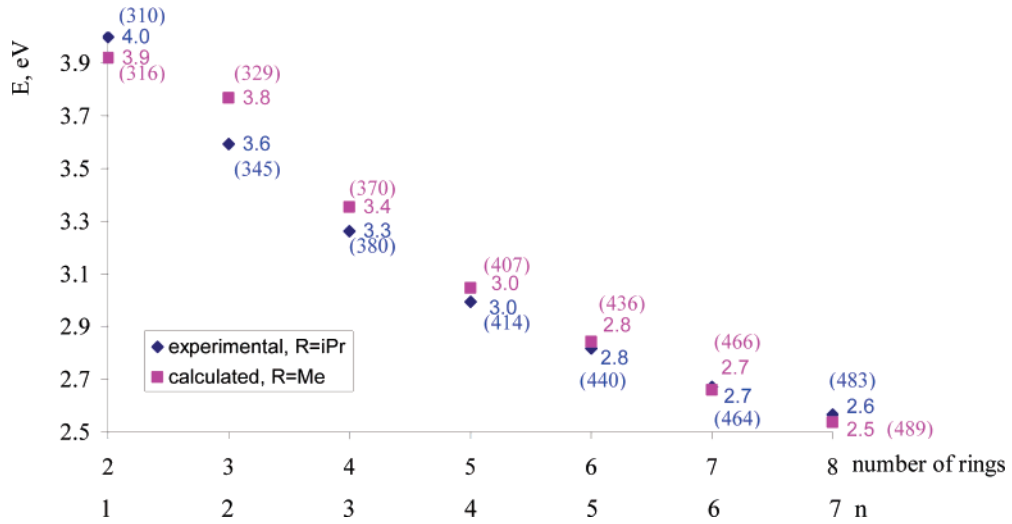

Figure 5. Lowest UV transition energies in eV (values in parentheses are given in nm) of **2** (n = 1−7) (calculated, TDB3LYP/6-311++G(d,p)//B3LYP/6-31G(d)) and **4** (n = 1−7) (measured).

Comparison between the helicity indexes of **2** (n = 1−4) and **2**$^{\bullet-}$ (n = 2−4) reveals that the helicity becomes smaller upon one-electron reduction of the ladder polysliane. For **2**$^{\bullet-}$ (n = 1−4) h is 8.9, 8.0, 22.6, and 23.3° (Figure 4), while h is 20.0, 33.6, 40.9, and 53.6° for **2** (n = 1−4) (Table 2, entry 9).

The ESR spectra of **4**$^{\bullet-}$ radical anions showed a relatively broad signal. The satellites were attributed to the ^{13}C nuclei of the *i*Pr groups rather than the ^{29}Si nuclei, and the number of spin couplings was equal to the number of equivalent carbon atoms, indicating that the spin is highly delocalized, in agreement with the shape of the LUMO (Figure 1).

We have calculated also the still unknown anion radicals **2**$^{\bullet-}$ (n = 5, 6). Comparison of the bond lengths and h values of **2** (n = 5, 6) and **2**$^{\bullet-}$ (n = 5, 6) reveals the same trends found for their shorter analogues, elongation of the longitudinal Si−Si bonds, shortening of the bridging Si−Si bonds, and a decrease of h upon one-electron reduction (h is reduced from 66.7° in **2** (n = 5) to 39.1° in **2**$^{\bullet-}$ (n = 5) and from 74.8° in **2** (n = 6) to 52.2° in **2**$^{\bullet-}$ (n = 6)).

4. UV Spectra of Alkyl-Substituted Ladder Polysilanes. The calculated (TDB3LYP/6-311++G(d,p)//B3LYP/6-31G(d,p)) lowest energy electron transitions of methyl-substituted ladder polysilanes are shown in Figure 5. The lowest electronic energy transition, measured experimentally, decreases from 4.0 eV in **4** (R = *i*Pr, n = 1) to 2.6 eV for **4** (R = *i*Pr, n = 7).[8] These values are in very good agreement with the calculated lowest energy transitions in **2** (n = 1−7), where the transition energy drops from 3.9 eV in **2** (n = 1) to 2.5 eV for **2** (n = 7). This decrease in the transition energy is consistent with the calculated decrease in the HOMO−LUMO gap from 4.8 eV in **2** (n = 1) to 3.2 eV for **2** (n = 7) (Figure 6).[28a] The extrapolation of the UV transition energies to the polymeric limit predicts UV transition energies of 2.3 and 2.1 eV for **2** (R = Me, calculated) and **4** (R = *i*Pr, experimental),[28b] respectively, considerably smaller than the value of 4.2 eV (295 nm) measured for polydimethylsilane.[1a]

The conformation of the ladder polysilane has a strong effect

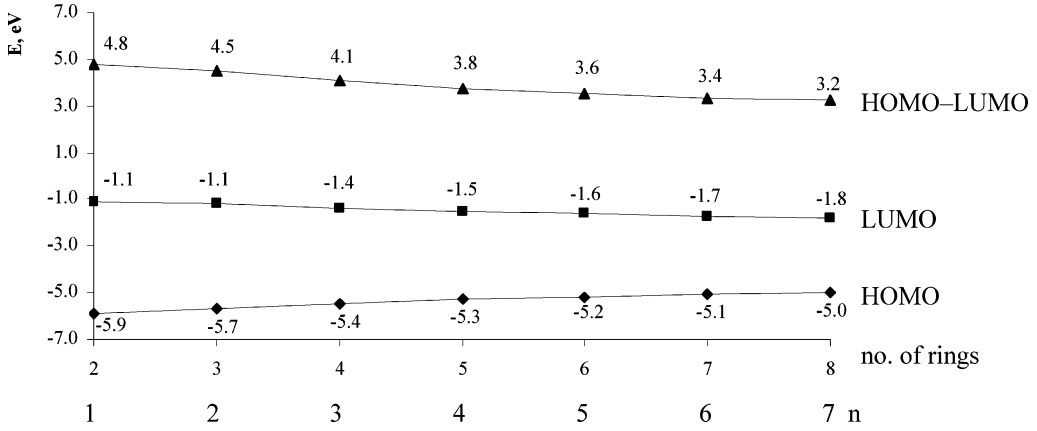

Figure 6. Calculated HOMO and LUMO energies (eV)[21a,b] and the HOMO−LUMO gap of **2** (n = 1−7) (B3LYP/6-311++G(d,p)//B3LYP/6-31G(d)**)**.

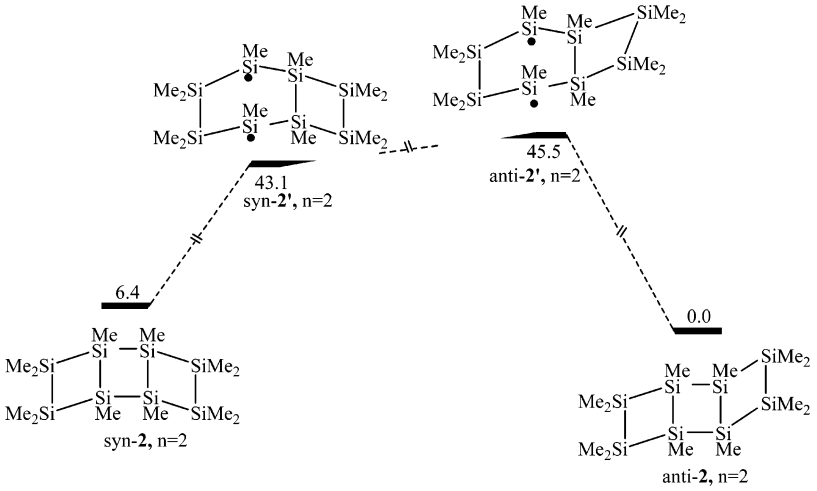

Figure 7. Calculated reaction path (only minima, at UB3LYP/6-31G(d)//UB3LYP/6-31G(d)) for the thermal isomerization of *syn*-**2** (n = 2) to *anti*-**2** (n = 2). Energies are given in kcal/mol (not including zero point energy corrections).

on the UV transition. Thus, the calculated energy for the lowest UV transition for *syn*-**2** (n = 2) is 3.3 eV (374 nm), 0.5 eV lower than for the corresponding anti isomer. This computational finding is in good agreement with the experimentally measured values for *syn*-**4** (n = 2) of 3.1 eV (398 nm) and for *anti*-**4** (n = 2) of 3.6 eV (345 nm). The lowest UV transitions are also consistent with the calculated HOMO−LUMO gaps of 4.1 eV in *syn*-**2** (n = 2) and 4.6 eV in *anti*-**2** (n = 2) (see Scheme 1 for the syn and anti conformations).

5. Thermal Rearrangement of Syn to Anti Ladder Polysilanes. At 220 °C *syn*-**4** (n = 2) rearranges quantitatively to its anti isomer (Scheme 1). Kinetic studies showed that this is a unimolecular process with an activation energy of 42.3 kcal/mol and a very small activation entropy of 0.0076 kcal mol^{-1} K^{-1}.[8a,b] The high activation energy was attributed to the cleavage of one of the bridging Si−Si bonds, leading to formation of a biradical intermediate.[8a,b]

To understand the mechanism of the isomerization of *syn*-**4** (n = 2) to *anti*-**4** (n = 2) (Scheme 1), we studied computationally the isomerization of the model *syn*-**2** to *anti*-**2**. The calculations predict that *anti*-**2** is more stable than the *syn*-**2** isomer by 6.4 kcal/mol. The calculated (at UB3LYP/6-31G(d)//UB3LYP/6-31G(d)) isomerization reaction path involves two biradical intermediates, *syn*-**2′** and *anti*-**2′**, as shown in Figure 7. The *syn*-**2′** biradical intermediate, which results from cleavage of one of the bridging Si−Si bonds, is 36.7 kcal/mol higher in energy than *syn*-**2**. The syn biradical isomerizes to the anti isomer, *anti*-**2′**, which is 2.4 kcal/mol higher in energy. In the final step, *anti*-**2′** collapses to *anti*-**2**, which is 45.5 kcal/mol lower in energy. Thus, the activation barrier for the rearrangement of *syn*-**2** to *anti*-**2** is estimated by the calculations to be at least 39.1 kcal/mol. This estimation[29] is in good agreement with the experimental barrier of 42.3 kcal/mol.[8a,b]

Scheme 1

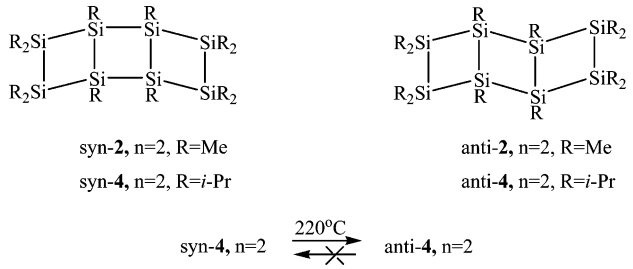

The calculated Si−Si σ bond energy in *syn*-**2** of 36.7 kcal/

(28) (a) The calculated HF/6-31G(d)//B3LYP/6-31G(d) values of the HOMO−LUMO gaps of **2** (n = 1−4) are 10.7, 10.2, 9.6, and 9.1 eV, respectively, much higher than those calculated at B3LYP/6-311++G(d,p)//B3LYP/6-31G(d), and differ significantly from the calculated UV transitions of **2** and from the measured values of **4**. (b) The graph that describes the correlation between the UV transition energies and the reciprocal of the number of repeat units n (1/n) for **2** and **4** (n = 2−7) fits a quadratic function well (R^2 = 0.999). For details see Figure 2S in the Supporting Information.

mol is significantly lower than a regular Si−Si bond energy of 70.5 kcal/mol.[30] We suggest that this large difference in the Si−Si bond energy between *syn*-**2** and regular Si−Si bonds is due to stabilization of the 1,4-biradical by through-bond conjugation with the two Si−Si σ bonds connecting the two radical centers. Such through-bond conjugation is absent when a regular Si−Si bond is cleaved into two separate silyl radicals. Substitution by α-silyl groups, as in **6**, stabilizes the silicon radical center but the stabilization is much smaller than for **2′**: i.e., the Si−Si bond dissociation energy (calculated at UB3LYP/6-31G(d)//UB3LYP/6-31G(d)) for the cleavage of the central Si−Si bond in **5** to yield the corresponding silyl radicals **6** is 64.0 kcal/mol (eq 2).

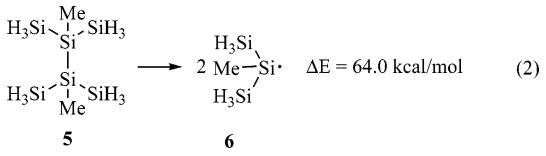

Scheme 2

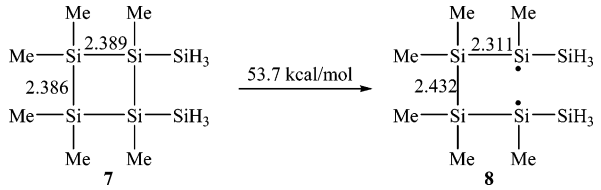

A closer model to the cleavage of the central bond in **2′** ($n = 2$) is provided by **7** (Scheme 2), for which the calculated energy for the Si−Si bond cleavage is 53.7 kcal/mol. This bond energy lies between that of the ladder polysilane *syn*-**2** ($n = 2$) at 36.7 kcal/mol (Figure 7) and that of **5** at 64.0 kcal/mol. Biradical **8** is stabiblized relative to **6** by through-bond interaction of the 1,4-biradical. This is evident from the shortening of the two Si−Si bonds to 2.311 Å and elongation of the central σ bond to 2.432 Å relative to corresponding bonds of 2.389 and 2.386 Å in **7** (Scheme 2). In **2** the Si−Si bond cleavage is still lower than in **7**, probably due to a relief of strain in going from **2** to **2′**.

Summary and Conclusions

Density functional calculations for a series of ladder polysilanes constituting up to eight tetrasilacyclobutane rings are reported. The parent systems (with hydrogen substitution) **1**, with $n > 3$, have essentially planar four-membered rings and the ladder skeleton does not form a helix. The silicon ring skeleton twists upon substitution of hydrogens by CH_3 or SiH_3 substituents, thus forming a double-helix structure, in agreement with the experimentally determined structures of **4** (R = *i*Pr). The puckering of each of the rings does not change significantly upon chain elongation, but the sum of the dihedral angles of the rings leads eventually to a helical ladder polysilane. It is predicted that ladder polysilanes with ca. 15 tetrasilacycobutane rings, not yet known experimentally, complete a full turn of the helix.

Ladder polysilanes show electronic properties similar to those of oligosilanes: e.g., destabilization of the HOMO and stabilization of the LUMO, leading to a reduced HOMO−LUMO gap upon chain elongation. The calculated UV lowest transitions ranging from 3.9 eV (316 nm) for **2** ($n = 1$) to 2.5 eV (489 nm) for **2** ($n = 7$) are in very good agreement with the experimentally measured values. The electronic structure and shape of orbitals of ladder polysilanes is discussed. Calculations support the experimental suggestion that the thermal syn−anti isomerization of *syn*-**4** ($n = 2$) to *anti*-**4** ($n = 2$) proceeds via biradical intermediates. A similar mechanism should hold for syn−anti isomerization of other ladderanes.

The general good agreement that we find between calculated and experimental data demonstrates that density functional calculations combined with a moderate basis set can be used reliably to predict both the geometry and the electronic properties of yet unknown longer chain ladder polysilanes. The effect of substituents which can interact with the HOMO and LUMO, such as π electron acceptors and π electron donors, thus lowering their relative energies, can be also studied reliably. In view of the recent experimental achievements in the synthesis of long-chain ladder polysilanes, we are studying computationally[31] the possibility that ladder polysilanes can exhibit fluxional behavior via Cope rearrangements, analogous to the case for carbon ladderanes, which have recently attracted much interest.[14a]

Acknowledgment. This paper is dedicated to Prof. Mitsuo Kira with friendship and deep appreciation for his many important contributions to silicon chemistry. This research was supported by the Minerva Foundation in Munich and by the U.S.-Israel Binational Science Foundation (BSF).

Supporting Information Available: Tables giving Cartesian coordinates, total energies, and ZPE values for all calculated species, Tables 1S and 2S, which show the dependence of the helicity and HOMO−LUMO gaps on the size of the basis set, and Figures 1S and 2S, showing plots of HOMO−LUMO gaps and UV lowest transition energies vs 1/*n*. This material is available free of charge via the Internet at http://pubs.acs.org.

OM0610344

(29) This work will be published elsewhere.

(30) (a) Transition states were not located. (b) The reliability of the UB3LYP energies for calculating singlet 1,4-biradicals was tested for the model biradical **1** (R = H, $n = 1$) by comparison with several high-level ab initio and DFT methods. Similar trends in the relative energies of bicyclic **1** ($n = 1$) and of biradical **1′** (R = H, $n = 1$) were calculated by DFT or ab initio methods. For example, the biradical **1′** (R = H, $n = 1$) lies 47.6, 45.8, and 31.9 kcal/mol above the bicyclic **1** (R = H, $n = 1$) at UB3LYP/6-31G(d)//UB3LYP/6-31G(d), UMP2/6-31G(d)//UMP2/6-31G(d) and CAS-(6,6)/6-31G(d)//CAS(6,6)/6-31G(d) levels of theory, respectively. We have also found that the UB3LYP/6-31G(d) and UB3LYP/6-311+G(3d) geometries and relative energies of all the species on the PES for the isomerization of *syn*-**1** (R = H, $n = 2$) to *anti*-**1** (R = H, $n = 2$) (closed shell and biradicals) are very similar, justifying the use of the smaller basis set for **2** (R = Me, $n = 2$). (c) The UB3LYP/6-31G(d) $\langle S^2 \rangle$ expectation value is 0.9 for both *syn*-**2′** and *anti*-**2′**. Since the energies of triplet *syn*-**2′** and *anti*-**2′** are very close to those of the pure singlet state energies, the energies calculated for pure and contaminated wave functions are nearly the same (energy difference of ca. ±0.2 kcal/mol). For a formula of how to calculate the energy of a pure singlet state and a discussion see: Gräfenstein, J.; Hjerpe, A. M.; Kraka, E.; Cremer, D. *J. Phys. Chem. A* **2000**, *104*, 1748.

(31) (a) For calculated Si−Si bond energies see: Karni, M.; Apeloig, Y.; Kapp, J.; Schleyer, P. v. R. In *The Chemistry of Organic Silicon Compounds*; Rappoport, Z., Apeloig, Y., Eds.; Wiley: Chichester, U.K., 2001; Vol. 3, Chapter 1, p 1. (b) For experimental Si−Si bond energies see: Walsh, R. In *The Chemistry of Organic Silicon Compounds*; Patai, S., Rappoport, Z., Eds.; Wiley: Chichester, U.K., 1989; Chapter 5, p 371.